Cationic and Anionic Fragmentation of Dichloromethane following Inner-Shell (Cl 1s) Photoexcitation

A. F. Lago,*,†,‡ J. Z. Dávalos,§ U. Kerdpin,∥,⊥ and A. S. Schlachter∥

Department of Chemistry, University of North Carolina, Chapel Hill, North Carolina 27599-3290, Laboratório Nacional de Luz Síncrotron, Box 6192, Campinas, SP, 13084-971, Brazil, Instituto de Quimica-Fisica "Rocasolano", CSIC, Serrano 119, 28006, Madrid, Spain, Advanced Light Source, Lawrence Berkeley National Laboratory, Berkeley, California 94720, and Faculty of Science, Naresuan University, Phitsanulok 65000, Thailand

Received: June 2, 2006; In Final Form: October 25, 2006

The cationic and anionic fragmentation of dichloromethane (CH_2Cl_2) molecule have been investigated in the energy range of the Cl K shell by using synchrotron radiation, ion yield spectroscopy, and electron−ion coincidence spectroscopy. Total and partial ion-yield and mass spectra have been recorded as a function of the photon energy. We were able to identify several singly and multiply charged cationic fragments and the following anionic species: H^-; C^-; Cl^-. The present results provide the first experimental report of negative ion formation from a molecule excited at the Cl 1s edge. In addition, our electron−ion coincidence data provide strong evidence of the preservation of molecular alignment for the photodissociation of CH_2Cl_2 after deep core−electron resonant excitation.

1. Introduction

Excitation of an inner-shell electron in a molecule usually results in fragmentation during or after the process of electronic relaxation. The main observed mechanism is the decay of the highly excited species to form singly or multiply charged species, depending on the available excess energy. Generally, at energies below threshold, the final states appear mostly as singly charged species, while above threshold the multiply charged species usually dominate. Core−electron excitation to an unoccupied orbital may also be followed by simultaneous valence excitations resulting, for instance, in doubly excited states. Such states usually exhibit characteristic resonance features in the region of the photoionization continuum, which is also the region where shape resonances are characteristically observed.

The formation of ion pairs (positively and negatively charged species) has been long known.[1−5] It occurs especially in the vicinity of the ionization thresholds, where these ionic pairs are mostly created after resonant excitation of neutral states. Dujardin et al.,[4] for instance, reported the first experimental evidence of ion-pair formation from the core-excited sulfur dioxide molecule, measured using synchrotron radiation and ion yield spectroscopy. They have demonstrated in that work that negative ions are produced both in the direct double photoionization region and also following core excitation. Suzuki et al.[5] have also observed ion-pair formation from a set of halomethane molecules (CH_3X, X = F, Cl, Br) photoexcited in the valence region.

Ion yield spectroscopy and synchrotron radiation have been recently employed as a powerful combination for investigating molecular process occurring at core-excited levels. It has been suggested that cation and anion yield spectroscopy can be used as an important experimental tool in differentiating above-threshold double-excitation processes from shape resonances. At least in small molecules, shape resonances are unlikely to result in anion production because they would initially undergo a normal Auger decay to yield a doubly charged state, and if it had to yield an anion, that would require the less probable corresponding formation of a triply charged positive ion or sufficient smaller positive ions to give the same net charge. Several small core excited molecules have been successfully investigated using this method.[6−11] However, a recent study of the SF_6 molecule excited around the S 2p and F 1s edges[12] indicates that this generalization may not hold for larger molecular systems, because additional ways of delocalizing the positive charge and produce anions would be available at shape resonances, contrary to what has been observed for small molecules. In another recent work Scully et al.[13] reported negative photoion fragments from Freon molecules in the vicinity of the shallow core Cl 2p level.

Halogenated methane derivatives form an interesting group of molecules to study. Molecules of this family have been observed quantitatively in the troposphere and have consequently been considered important sources of reactive halogens in atmosphere. Furthermore, from a fundamental viewpoint, the investigation of the photoionization and fragmentation processes involving halogenated compounds have also attracted recent experimental and theoretical interest as a result of the variety of dissociation channels and species which can be identified upon absorption of VUV and X-ray photons.[14−20]

This work is dedicated to the study of the cationic and anionic photoinduced fragmentation of the CH_2Cl_2 molecule using ion yield spectroscopy, time-of-flight mass spectrometry (TOF-MS) in the electron−ion coincidence modes (PEPICO and PEPI-

* To whom correspondence should be addressed. Present address: Laboratório Nacional de Luz Síncrotron (LNLS), Box 6192, Campinas-SP, 13084-971, Brazil. E-mail: alago@lnls.br.
† University of North Carolina.
‡ Laboratório Nacional de Luz Síncrotron.
§ Instituto de Quimica-Fisica "Rocasolano", CSIC.
∥ Lawrence Berkeley National Laboratory.
⊥ Naresuan University.

10.1021/jp063423h CCC: $33.50
Published on Web 12/21/2006

PICO), and synchrotron radiation following deep core-level photoexcitation in the vicinity of the Cl 1s edge (2810−2860 eV). Within our knowledge, no similar study has been reported in the literature for this molecule.

2. Experimental Section

The experiment was performed by using synchrotron radiation from the 9.3.1 beamline at the Advanced Light Source (ALS), Berkeley, CA. This beamline is based on a bending magnet which provides X-ray photons in the 2−6 keV energy range. The experimental apparatus used in this work has been described in detail elsewhere.[21] It basically consists of a 180° magnetic sector mass spectrometer, an electrostatic lens to focus the ions created in the interaction region onto the entrance slit of the spectrometer, and an effusive-jet gas cell containing push and extraction plates to move the ions from the interaction region into the lens. Ions are detected with a channel electron multiplier (CEM) at the exit slit of the spectrometer. The polarity of the lens, the magnetic field, and the CEM may be switched to allow detection of either cations or anions produced in the interaction region. This spectrometer has a mass-to-charge resolution of approximately 1 part in 50. During the experiment, the pressure was maintained below 10^{-5} Torr (background was 10^{-8} Torr), and the gas needle was kept at ground potential. The total and partial ion yield spectra were obtained by scanning the photon monochromator through the Cl K-edge region while monitoring the ion signal. The mass calibration for the ion yield spectra was made by means of an empirical equation, $V_{mag} = [(m/z)/c]^{1/2}$, which relates the potential applied to the instrument magnets (V_{mag}) with the corresponding mass/charge of the selected ions, and c is a constant related to the instrument settings. This calibration procedure has been tested with different molecular systems and presented a satisfactory precision. Although the chlorine 35 isotope is the one used in the determination of the PIY, the Cl (37) isotope contribution was also taken into account in the determination of the ionic fragments involving chlorine in the PIY spectra to locate and assign eventual overlapping structures due to the relatively low experimental resolution of the magnetic sector spectrometer. Recent improvements made to the 9.3.1 ALS beamline and experimental apparatus allowed the observation of lower intensity fragments than had previously been observed. The photon energy was calibrated using the measured spectrum of the CF_3Cl molecule, which presents a known resonance at 2823.4 eV.[22] The total and partial ion yield spectra were normalized to the photon flux and sample pressure. The CH_2Cl_2 sample was commercially obtained from Sigma-Aldrich with 99.8% purity. No further purification was used except for degassing the liquid samples by multiple freeze−pump−thaw cycles before admitting the vapor into the chamber. The electron−ion coincidence experiments were performed using the soft X-ray spectroscopy beamline (SXS)[23] at the Laboratório Nacional de Luz Síncrotron (LNLS) in Brazil. This beamline operates in the 800−4000 eV energy range and provides a photon flux of approximately 10^{11} photons/s/100 mA/0.1% bandwidth and a resolving power better than 5000. Description on the time-of-flight spectrometer used in our experiments is given in the literature.[24] Briefly, the TOF spectrometer, mounted inside a vacuum chamber, present a cylindrically symmetric geometry with respect to the ion extraction region. The molecules in the form of a collimated gas jet interact perpendicularly with the synchrotron light at the center of the ionization region and are excited/ionized giving rise to photo- or Auger electrons as well as ions which may further fragment. Electrons are attracted toward the electron micro channel plate (MCP) and detected, without kinetic energy analysis, providing a start signal to the experiment. Positive ions are attracted in opposite direction and detected by the ion MCP which provides the stop signals to the time-to-digital converter (TDC). The apparatus is designed to follow the Wiley−McLaren conditions.[25] Two grids are used to define the extraction region, and lenses are mounted to provide enhanced electron and ion detection efficiencies. A 766 V/cm dc electric field is applied to the first acceleration region. The time-of-flight spectrometer was designed to present no angular discrimination of the ejected ions with kinetic energy release up to 40 eV. The electron−ion coincidence experiments (PEPICO and PEPIPICO) have been performed with TOF drift tube oriented linearly relative to the plane of polarization of the synchrotron light.

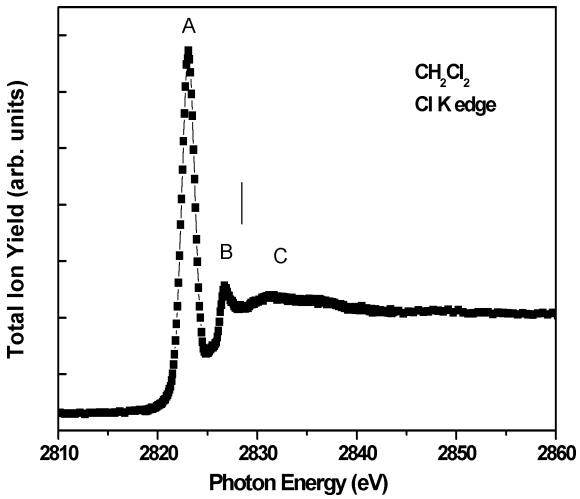

Figure 1. Total ion yield spectrum for CH_2Cl_2 in the vicinity of the Cl K edge. The vertical line represents the approximate Cl 1s ionization threshold.

The experimental techniques used in this work are capable of providing complementary results. In the partial ion yield experiment, using a magnetic sector apparatus, one can select a single ionic fragment at a time and record is intensity as the photon energy is scanned. In the coincidence experiment, on the other hand, all ions generated from the dissociative photoionization process at a single selected energy at a time are collected and separated according to their mass to charge ratios within a defined time window.

3. Results and Discussion

3.1. Total and Partial Ion Yield. The dichloromethane molecule belongs to the C_{2v} symmetry point group in its ground electronic state ($X\ ^1A_1$) and possess the 20 outermost valence electrons distributed in 10 molecular orbitals as the following configuration: $[6a_1]^2\ [5b_2]^2\ [7a_1]^2\ [2b_1]^2\ [8a_1]^2\ [6b_2]^2\ [2a_2]^2\ [9a_1]^2\ [7b_2]^2\ [3b_1]$.[2] The core electrons, which present mostly atomic character, are distributed as Cl 1s $\{[1b_2]^2\ [1a_1]^2\}$, C 1s $\{[2a_1]^2\}$, Cl 2s $\{[2b_2]^2\ [3a_1]^2\}$, Cl 2p $\{[3b_2]^2\ [4a_1]^2\ [4b_2]^2\ [5a_1]^2\ [1a_2]^2\ [1b_1]^2\}$. The lowest unoccupied molecular orbitals are $[10a_1]^0\ [11a_1]^0\ [4b_1]^0\ [4b_2]^0$. This electronic configuration was computed from ab initio calculations (MP4/6-311G** full level of theory) using the Gaussian 03 package.[26]

The total ion yield spectrum of the CH_2Cl_2 molecule, which strongly resembles a near-edge X-ray absorption spectrum (NEXAFS), has been measured as a function of the photon energy (2810−2860 eV), around the chlorine K edge, and is presented in Figure 1. It shows an intense peak observed at

2823.2 eV, indicated by A, which has been associated with an electronic transition to an unoccupied antibonding character molecular orbital (Cl 1s → σ^*), in which the most conceivable is a transition to the unoccupied a_1 orbital. From the molecular orbital population analysis, obtained from our ab initio calculations, we were able to observe that the LUMO a_1 molecular orbital presents a mixed-valence character with strong carbon 4s orbital coefficient, whereas the lowest unoccupied b_1 and b_2 orbitals, which have approximately the same energy, present important carbon 4p orbital coefficients. The feature indicated by B located near the Cl 1s ionization threshold (∼2828.6 eV)[27] is most likely associated with electronic transitions involving mixed Rydberg/valence character states. The structures observed above the Cl 1s ionization edge indicated by C have been attributed mainly to contributions from doubly excited states, as also observed for small chlorine-containing molecules,[28] but some contribution from shape resonances may also be expected.

The total ion yield spectrum of CH_2Cl_2 differs from those reported for the $CHCl_3$[16] and CCl_4[29] molecules. One additional peak, which is not clearly observed in Figure 1, located in a corresponding position between peaks A and B, is on the other hand clearly observed for both $CHCl_3$ and CCl_4 molecules. It has been suggested, for the latter molecule,[29] that this intermediate feature corresponds to a splitting for the Cl 1s → σ^* resonance due to the energy difference between a_1 and t_2 orbitals (T_d symmetry). The TIY spectrum for $CHCl_3$ (C_{3v}) also presents this structure which may be attributed to the energy difference between the unoccupied a_1 and e orbitals. In the case of CH_2Cl_2 (C_{2v}), the Cl 1s $1b_2$ and $1a_1$ orbitals are degenerate and the energy difference for the lowest unoccupied a_1 and b_2 orbitals is about 1.7 eV, according to our ab initio calculations. However, this intermediate feature at about 2825 eV is either very weak or absent from the TIY spectrum shown in Figure 1. As expected, the spectrum for the CH_3Cl[30] does not show such feature because there is no splitting in the Cl 1s → σ^* resonance for this molecule.

The partial ion yield spectra for all detectable singly charged cationic fragments from CH_2Cl_2 are presented in Figure 2, as a function of photon energy. The following species have been observed: H^+; Cl^+; C^+; CH^+; HCl^+; CH_2^+; CCl^+. The most important contribution to the singly charged ion yield comes from the Cl^+ ion, followed by CH_2^+ and C^+ fragments. These ions are formed with significant intensity at the main resonance about 2823.2 eV, which is a demonstration of its strong dissociative character. However, the spectra for the other singly charged fragments in Figure 2 present increasing contributions from the features near the ionization threshold (∼2827 eV) and in regions above the ionization threshold. It should also be noted from Figure 2 the observation of the stable (in the time frame of the experiment) rearrangement product HCl^+ with low intensity and the C^+ which is a signature of the complete atomization of the molecule. Another interesting observation concerns the CH_2^+ fragment, which is mostly produced at the main resonance, and may be an evidence of site-selective fragmentation.

From the comparison of the present results with the ones previously reported for $CHCl_3$[16] and CH_3Cl,[30] we note that the production of singly charged atomic fragments H^+, Cl^+, and C^+ is common to all molecules. As for the molecular ions, despite the possibility of forming species such as CCl^+, CH^+, and HCl^+ (rearrangement) singly charged fragments, none have been observed for all three molecules upon Cl 1s excitation, which is an indication of the different fragmentation pathways associated with these molecules.

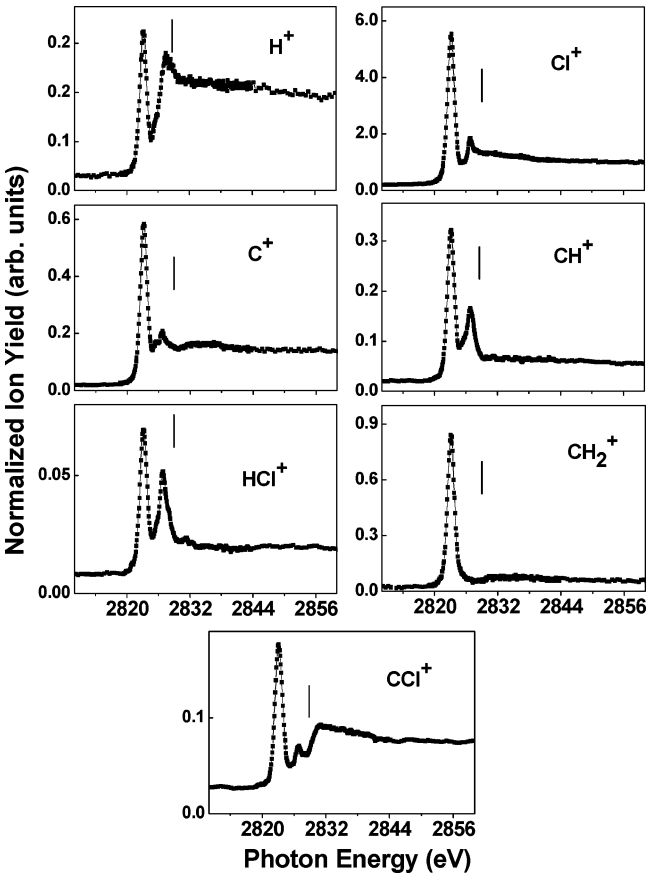

Figure 2. Partial ion yield spectra for singly charged cations.

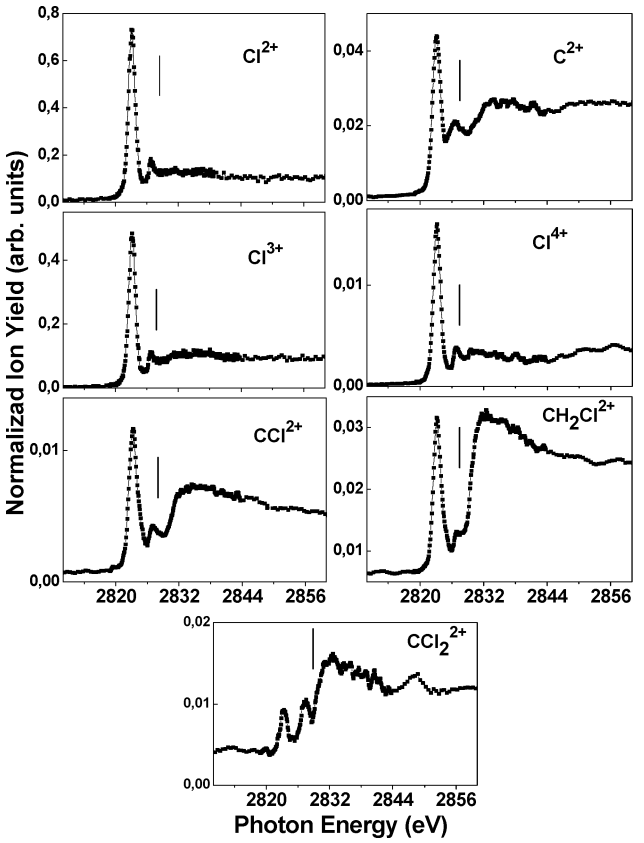

Figure 3. Partial ion yield spectra for multiply charged cations.

Figure 3 shows the individual contributions of several multiply charged cations formed from CH_2Cl_2. Atomic chlorine fragments with charges up to 4+ have been identified. The Cl^{4+}

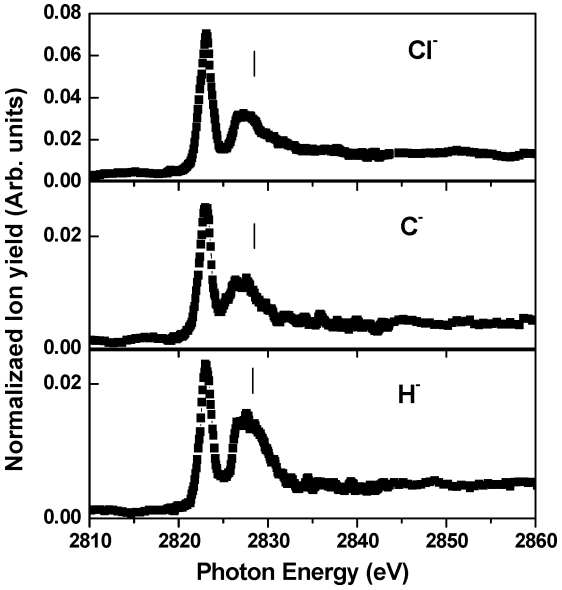

Figure 4. Partial ion yield spectra for negative ions.

and C^{2+} atomic fragments have not been detected in a previous study for the chloroform molecule,[16] albeit the C^{2+} fragment has also been observed on and above the Cl 1s resonance in the ion-coincidence spectra of CH_3Cl.[30] It is interesting to observe the striking differences in the spectra presented in Figure 3 for atomic fragments, mostly formed at the main resonance, in contrast to the molecular fragments which exhibit strong features above the ionization threshold, indicating that these fragments are formed via distinct decay mechanisms.

The partial anion yield spectra for all detectable fragments from CH_2Cl_2 as a function of the photon energy around the Cl K edge are shown in Figure 4. The following negative fragments have been identified: Cl^-; C^-; H^-. Although we have scanned through all possible anionic mass to charge ratio at several energies in search for molecular negative fragments, none have been detected for this molecule in this energy range. In addition, the much lower intensity for the production of negative ions as compared to the corresponding positive fragments should also be pointed out. The most intense anionic fragment from the dichloromethane molecule is attributed to the Cl^- ion, similarly to the Cl^+ fragment, which may be explained in part by the highly localized character of the inner-shell excitation in this energy range leading to an efficient C−Cl bond breaking. Also, the order of intensities for the negative ions observed in this work ($Cl^- > C^- > H^-$) proportionally follow the electron affinities for these species (3.61, 1.26, 0.76 eV),[31] respectively. The partial ion yield spectra for the negative fragments in Figure 4 show some similarities. These fragments are formed predominantly at both the main resonance at about 2823.2 eV and near the ionization threshold. However, we note that the structure near the ionization threshold seems to become relatively more important as we move from Cl^- to C^- and H^- anions. An additional observation concerns the relative intensities for the structure observed in the anion yield spectra at energies very close to the Cl 1s ionization threshold. These features were much less prominent in the spectra for the corresponding cationic species, especially for Cl^+ to C^+ ions.

It is also interesting to note the shape of the anion yield spectra in Figure 4 at energies just above the Cl 1s ionization threshold (2828−2834 eV), which exhibit a tail that extends a few electronvolts toward a mostly flat region. These shapes closely resemble those observed in cases where postcollision interaction[32−34] (PCI) plays a role. The PCI is an effect of energy exchange between charged particles, especially electrons, which usually arises from the complex dynamics of many-electron interaction, as is the case of the Auger effect. A photoelectron (slow) may be overtaken by a faster second Auger electron, which in turn is screened by the slower electron, causing an energy transfer from the slower electron to the Auger electron. The PCI theory thus predicts the possibility of recapture of the photoelectron by a neutral species under favorable conditions. It may seem reasonable to speculate that this effect could explain in part the structures observed near the ionization threshold in Figure 4 and, consequently, would be considered as an additional mechanism leading to the negative ion formation for dichloromethane.

One of the most likely mechanisms for the production of these anionic species may be attributed to the formation of ion pairs from the corresponding cations. If the core excited molecule undergoes resonant Auger decay, which can be either spectator or participator, it usually yields singly charged species that may dissociate into small charged or neutral fragments. At energies above the ionization threshold the dominating process is probably the normal Auger, which results in doubly charged species that are usually more unstable and fragment efficiently. Some of the likely fragmentation pathways leading to the anions are described below, although other mechanisms may also occur because quadruple ionizations are also energetically possible at this energy range:

$$\begin{aligned} CH_2Cl_2^{+} &\rightarrow CCl^{+} + H^{+} + Cl^{-} + H \\ &\rightarrow CH_2^{+} + Cl^{+} + Cl^{-} \\ &\rightarrow Cl^{2+} + Cl^{+} + C^{-} + H^{-} + H \\ &\rightarrow CH^{+} + Cl^{2+} + Cl^{-} + H^{-} \end{aligned} \quad (1)$$

$$\begin{aligned} CH_2Cl_2^{2+} &\rightarrow C^{+} + H^{+} + Cl^{+} + Cl^{-} + H \\ &\rightarrow C^{+} + H^{+} + H^{+} + Cl + Cl^{-} \\ &\rightarrow C^{+} + Cl^{2+} + H^{+} + Cl^{-} + H^{-} \\ &\rightarrow Cl_2^{+} + Cl^{+} + H^{+} + H^{-} + C^{-} \end{aligned} \quad (2)$$

$$\begin{aligned} CH_2Cl_2^{3+} &\rightarrow C^{+} + H^{+} + Cl^{2+} + Cl^{-} + H \\ &\rightarrow C^{+} + H^{+} + Cl^{+} + Cl^{-} + H^{-} \end{aligned} \quad (3)$$

Another interesting observation can be made from the comparison of the ion yield spectra for the positive C^+, Cl^+, and H^+ (Figure 2) and their corresponding anions C^-, Cl^-, and H^- (Figure 3). In general, the above-threshold structures for C^+, C^- and Cl^+, Cl^- are quite similar. However, we find important differences in the above-threshold shape for the H^+ and H^-, which seems to suggest the role of doubly excited states that decay mainly to the singly charged $CH_2Cl_2^+$ and may consequently dissociate via mechanisms (1) to efficiently produce H^- at energies above the Cl 1s ionization threshold.

We have also recently observed anion formation from the chloroform molecule at the Cl K edge, and the results will be presented elsewhere.

3.2. Electron−Ion Coincidence. The electron−ion coincidence techniques combined with synchrotron radiation are important tools for studying molecular dissociation and dynamics. In this work we have also performed electron−ion coincidence experiments for CH_2Cl_2 to confirm and supplement

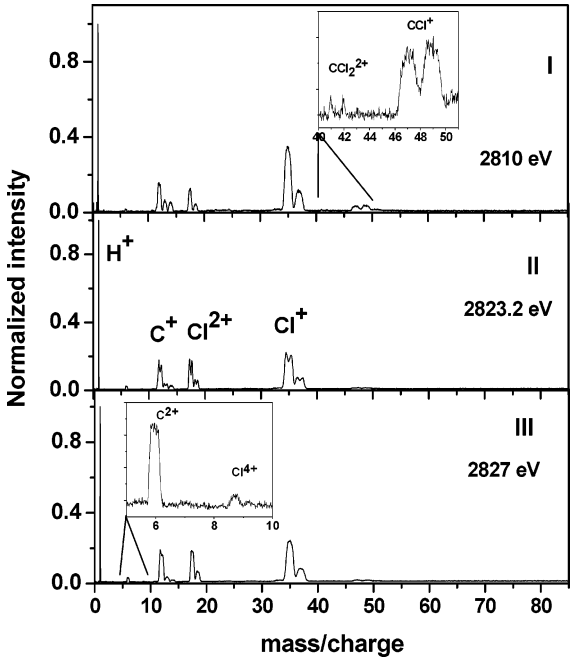

Figure 5. PEPICO spectra for CH_2Cl_2 at selected energies near the Cl 1s edge.

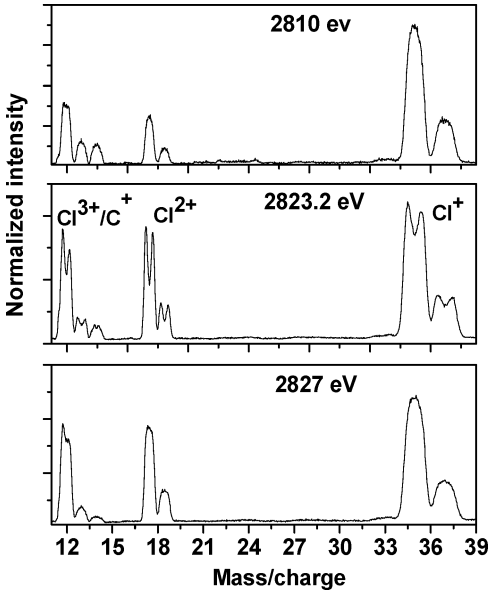

Figure 6. Enlargement of PEPICO spectra showing the fragment peak shape differences as a function of photon energy.

the results obtained via a different experimental technique, as reported in the previous section.

The PEPICO spectra (I−III) have been recorded at distinct energies along the Cl 1s edge and are shown in Figure 5, corresponding to positions before, on, and after the Cl 1s → σ^* resonance, respectively. From Figure 5 we confirm that no molecular ion $CH_2Cl_2^+$ ($m/z = 84$) is observed in this energy range. In addition, the dissociation channels leading to the H^+ fragment are, as expected, quite important and increase with energy along the Cl 1s edge. The insets in Figure 5 (I and III) show a magnification of the main low-intensity fragments C^{2+} ($m/z = 6$), Cl^{4+} ($m/z = 8.75$), CCl_2^{2+} ($m/z = 41$), and CCl^+ ($m/z = 47$) present in the spectra. These ions have also been detected by ion yield spectroscopy. Given the relatively low mass to charge resolution of the magnetic spectrometer used for the results in section 3.1, and the similarity in the shape of the ion yield spectra of C^+ and Cl^{3+} in Figures 2 and 3, it is not straightforward to separate the contributions from these species. However, by looking at the mass spectra in Figures 5 and 6 and taking into account the expected isotopic ratio for the Cl^{3+} ion, we can conclude that the dominant contribution to this peak comes from the Cl^{3+} fragment but with some contribution from C^+ ion. This explains the considerably lower yield of the C^+ as compared for instance to the Cl^+ in the partial yield (Figure 2). The low-intensity rearrangement fragment HCl^+ observed in the ion yield spectrum is not seen in the electron−ion coincidence spectra due to the much more intense and broad structures for the Cl (35/37) ion. However, the substantially different shape of the partial ion yield spectrum for this ion in Figure 2 as compared to all the other spectra provides definite evidence that this specie can in fact be formed via a less favorable fragmentation channels at selected energies near the Cl 1s edge.

The spectra presented in Figure 5 also show evidence of extensive molecular fragmentation in this energy range where the atomic fragments (H^+, Cl^{3+}, C^+, Cl^{2+}, Cl^+) dominate. This result corroborates with the discussion made in section 3.1. The PEPICO results also give support to the observation that no molecular anion is found for this molecule in the vicinity of the Cl 1s edge as well as to the proposed fragmentation pathways leading to the observed negative ions. From Figure 5 we also note that no striking difference in the relative abundance of the fragments is observed, although a decrease in the abundance of the Cl^+ and CCl^+ fragments relative to H^+, C^+, and Cl^{2+} is noted as the photon energy increases. A relatively small broadening in the peaks from spectrum I to III is observed and is mainly attributed to the increasing kinetic energy released in the dissociation process. However, this broadening is less prominent as compared for instance to what occurs in the vicinity of the Cl 2p edge for the $CHCl_3$ molecule.[15]

The most interesting observation from Figure 5 (II) comes from the peak splitting of the fragments at the energy corresponding to the Cl 1s → σ^* resonance, which have not been observed in the spectra recorded at other energies. Figure 6 shows the enlargement in the PEPICO spectra for the most intense fragments (except H^+) as a function of photon energy. This figure clearly shows a "Doppler type" splitting for the peaks in the PEPICO spectrum only at 2823.2 eV, to which we attribute to a possible effect of preservation of the molecular alignment in the resonant Cl 1s core excitation for this molecule.

It is known that the orientation of a molecule is reflected in the fragmentation products provided the time scale of the decay is similar to the rotational period of the molecule, according to the axial-recoil approximation.[35] Assuming that this approximation is valid, and if we consider that the dipole approximation can lead to the orientational selection of the molecule, then the electronic excitation probability for a transition depends on both the angle between the polarization vector of the light and the transition moment of the molecule, which in the present case would be directed along the C−Cl bond. If we consider the initial state as a 1s orbital, which is spherically symmetric, and a σ^* orbital excitation, then the excitation probability would be approximately given by $\alpha = \cos^2 \theta$, where θ is the angle between the electric field vector and the vector directed along the amplitude of the intermediate state orbitals.[36]

Gel'mukhanov et al.[37] have predicted that Doppler effect may occur when the resonant Auger spectrum resulting from the decay of repulsive core-excited states reflects both the molecular decay and that from the excited dissociation fragments. The existence of Doppler type splitting due to the ultrafast dissociation of core-exited molecules have also been previously reported for small molecules.[38,39] From multicoincidence experiments,

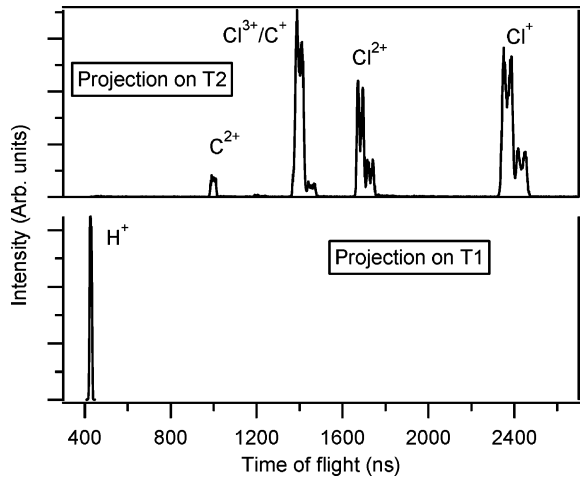

Figure 7. PEPIPICO projections for the double coincidences of H^+ ion at the Cl 1s resonance (2823.2 eV).

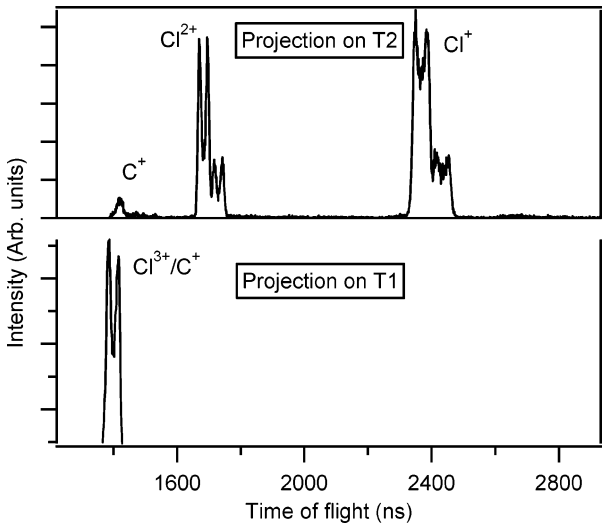

Figure 8. PEPIPICO projections for the double coincidences of Cl^{3+}/C^+ ions at the Cl 1s resonance (2823.2 eV).

Simon et al.[40] have observed a strong molecular alignment for the CS_2 molecule around the sulfur K edge. More recently, the effect of molecular quasi-alignment has been reported for polyatomic molecules by Lindgren et al.[41] and Mocellin et al.[42] using electron−ion−ion coincidence techniques.

The present results have been obtained with the TOF tube oriented at 0 deg with respect to the **E**-vector of the synchrotron light. In the case where the dissociation process is highly anisotropic and occurs along the light polarization vector, then the observation of this peak splitting would be likely, as observed in this work at the main resonance. On the other hand, we would expect that such splitting effect disappears if the experimental orientation is in a direction perpendicular with respect to the light polarization vector. This work provides strong evidence that the molecular alignment of CH_2Cl_2 is preserved upon resonant Cl 1s core−electron excitation and also seems to indicate that the Cl 1s $\rightarrow \sigma^*$ resonance exhibits an ultrafast dissociative behavior to the C−Cl bond. To our knowledge it is the first time that such molecular effect is reported for a molecule photoexcited at the Cl K edge.

To give further support to our conclusions, we have also included results from the electron−ion−ion coincidence (PEPIPICO) experiment recorded at the corresponding energy of the main Cl 1s resonance. The PEPIPICO data[43] reflects the time-of-flight of a pair of ions resulting from a dissociative ionization event which are detected simultaneously. It relates the arrival of two correlated ions during a selected time window after the detection of an electron from the ionization process. A PEPIPICO projection spectrum represents the yield of ions in coincidence with other charged species. Such spectrum may also contain contributions from triple or quadruple ionization where only two ions were detected.

Figures 7 and 8 show the projections from the main double coincidence channels resulting from the Cl 1s resonant photoexcitation and dissociation of CH_2Cl_2. In Figure 7 we observe that the H^+ ion forms coincidences with the ions C^{2+}, Cl^{3+}, C^+, Cl^{2+}, and Cl^+. Figure 8 shows the ions in coincidence with the Cl^{3+}/C^+ ions, since they represent overlapping structures in the PEPICO spectrum. It is interesting to note that the ratio of the low mass/charge fragments is more important in PEPIPICO projections than in the PEPICO spectrum (Figure 5). It indicates the importance of the many-body fragmentation processes. From Figure 8 we can confirm that the overlapping peak containing Cl^{3+}/C^+ ions is in fact dominated by the Cl^{3+} ion, as previously pointed out. In addition, we clearly observe the coincidence channel between the Cl^{3+} (faster ion) with the C^+ (slower ion), where the latter ion does not exhibit splitting. Another important confirmation comes from the fact that the PEPIPICO projections in Figures 7 and 8 also show the splitting in the chlorine peaks at the Cl 1s resonance. This additional evidence to corroborate with our previous assumptions of the preferential alignment in the fragmentation of this molecule upon deep-core resonant photoexcitation.

A further insight on fragmentation pathways for this molecule at the Cl 1s resonance may be understood if we take into account that after deep-core excitation and ionization an ultrafast decay process may also take place,[44] in a case where the 2p electrons participate in a way that one electron fills the core hole and a second electron is ejected. This process may be followed by a double Auger decay leading to quadruply charged ions which further fragment to form mostly atomic ions. The previous explanation is supported by the fact that no major differences are observed in the fragmentation pattern of CH_2Cl_2 if we compare the PEPICO spectra at 2823.2 and 2827 eV (Figure 5). At these energies, we believe that double Auger decay plays a role, but it is unlikely to occur at 2810 eV. From the observations in the PEPIPICO spectrum and the previously discussed assumptions, we can also point out to the probability of occurrence of other dissociation mechanisms involving the quadruple charged molecule in addition to the ones already suggested, as listed as following:

$$\begin{aligned} CH_2Cl_2^{4+} &\rightarrow C^+ + Cl^{3+} + H^+ + Cl^- + H \\ &\rightarrow C^+ + H^+ + Cl^{2+} + Cl^+ + H^- \\ &\rightarrow H^+ + Cl^{3+} + H^+ + Cl^- + C \\ &\rightarrow H^+ + H^+ + Cl^{2+} + Cl^+ + C^- \end{aligned} \quad (4)$$

New electron−ion−ion coincidence (PEPIPICO) experiments are proposed including the use of different light polarization angles (by rotating our apparatus with respect to the incoming light) to further address the effect of molecular alignment for this molecule upon deep-core excitation.

4. Summary and Conclusions

The photofragmentation of the dichloromethane molecule has been investigated near the Cl K edge using ion yield spectroscopy, electron−ion coincidence, and synchrotron radiation. Total

and partial ion yield and mass spectra have been recorded as function of the photon energy. Positive (H^+, Cl^+, C^+, CH^+, HCl^+, CH_2^+, CCl^+, Cl^{2+}, Cl^{3+}, Cl^{4+}, C^{2+}, CCl^{2+}, CH_2Cl^{2+}, CCl_2^{2+}) and negative (Cl^-, H^-, C^-) fragments have been identified. Striking differences in the ion yield spectra for the anions have been observed and discussed in a comparative way. The spectra were dominated by atomic singly and multiply charged fragments. This work provides the first experimental report of negative ion formation from the dissociative photoionization of dichloromethane molecule following excitation in the vicinity of the Cl K shell. The fragmentation processes were governed by complex decay mechanisms involving singly and multiply charged species formed below and above the ionization threshold, as well as via dissociation into ion pairs. Several fragmentation pathways have been proposed from the analysis of the PIY and mass spectra. Our PEPICO and PEPIPICO results supplemented the analysis and assignment obtained from the ion yield spectra and also presented for the first time clear evidence of preservation of molecular alignment for the CH_2Cl_2 molecule upon resonant core−electron excitation at the Cl K shell.

Acknowledgment. We thank the ALS staff for their assistance during the experiments and especially Dr. W.C. Stolte for the use of his end station. We also thank the LNLS staff for the technical support. A.F.L. acknowledges the financial support from CNPq and FAPESP (Brazil) and the UNC chemistry department. J.Z.D. acknowledges the support of Spanish MEC Project BQU2003-05827. This work was supported by the Director, Office of Science, Office of Basic Energy Sciences, of the U.S. Department of Energy under Contract No. DE-AC02-05CH11231.

References and Notes

(1) Berkowitz, J.; Chupka, W. A. *J. Chem. Phys.* **1966**, *45*, 1287.
(2) Dehmer, P. M.; Chupka, W. A. *J. Chem. Phys.* **1975**, *62*, 4525.
(3) Berkowitz, J. *VUV and Soft X-Ray Photoionization*; Becker U., Shirley, D. A., Eds.; Plenum: New York, 1996.
(4) Dujardin, G.; Hellner, L.; Olsson, B. J.; Besnard-Ramage, M. J.; Dadouch, A. *Phys. Rev. Lett.* **1989**, *62*, 745.
(5) Suzuki, S.; Mitsuke, K.; Imamura, T.; Koyano, I. *J. Chem. Phys.* **1992**, *96*, 7500.
(6) Yu, S.-W.; Stolte, W. C.; Ohrwall, G.; Guillermin, R.; Piancastelli, M. N.; Lindle, D. W. *J. Phys. B: At. Mol. Opt. Phys.* **2003**, *36*, 1255.
(7) Stolte, W. C.; Ohrwall, G.; Sant'Anna, M. M.; Domingues Lopez, I.; Dang, L. T. N.; Piancastelli, M. N.; Lindle, D. W. *J. Phys. B: At. Mol. Opt. Phys.* **2002**, *35*, L253.
(8) Stolte, W. C.; Hansen, D. L.; Piancastelli, M. N.; Domingues Lopez, I.; Rivzi, A.; Hemmers, O.; Wang, W.; Schlachter, A. S.; Lubell, M. S.; Lindle, D. W. *Phys. Rev. Lett.* **2001**, *86*, 4504.
(9) Stolte, W. C.; Guillermin, R.; Wolska, A.; Feng, R.; Tran, I. C.; Lindle, D. W. *J. Electron Spectrosc. Relat. Phenom.* **2005**, *144*−*147*, 157.
(10) Stolte, W. C.; Sant'Anna, M. M.; Ohrwall, G.; Domingues Lopez, I.; Piancastelli, M. N.; Lindle, D. W. *Phys. Rev. A* **2003**, *68*, 2.
(11) Guillermin, R.; Stolte, W. C.; Dang, L. T. N.; Yu, S. W.; Lindle, D. W. *J. Chem. Phys.* **2005**, *122*, 94318.
(12) Piancastelli, M. N.; Stolte, W. C.; Guillermin, R.; Wolska, A.; Yu, S. W.; Sant'Anna, M. M.; Lindle, D. W. *J. Chem. Phys.* **2005**, *122*, 94312.
(13) Scully, S. W. J.; Mackie, R. A.; Browning, R.; Dunn, K. F.; Latimer, C. J. *Phys. Rev. A* **2004**, *70*, 042707.
(14) Lago, A. F.; Kercher, J. P.; Bodi, A.; Sztaray, B.; Miller, B. E.; Wurzelmann, D.; Baer, T. *J. Phys. Chem. A* **2005**, *109*, 1802.
(15) Lago, A. F.; Santos, A. C. F.; de Souza, G. G. B. *J. Chem. Phys.* **2004**, *120*, 9547−9555.
(16) Lago, A. F.; Santos, A. C. F.; Schlachter, A. S.; Stolte, W. C.; de Souza, G. G. B. *J. Electron Spectrosc. Relat. Phenom.* **2005**, *144*−*147*, 161.
(17) Sharma, P.; Vatsa, R. K.; Maity, D. K.; Kulshreshtha, S. K. *Chem. Phys. Lett.* **2003**, *382*, 637−643.
(18) Huang, J. H.; Xu, D. D.; Fink, W. H.; Jackson, W. M. *J. Chem. Phys.* **2001**, *115*, 6012−6017.
(19) Yang, G. H.; Meng, Q. T.; Zhang, X.; Han, K. L. Int. *J. Quantum Chem.* **2004**, *97*, 719−727. .
(20) Lago, A. F.; Baer, T. *Int. J. Mass Spectrom.* **2006**, *252*, 20−25.
(21) Stolte, W. C.; Yu, Y.; Samson, J. A. R.; Hemmers, O.; Jansen, D. L.; Whitfield, S. B.; Wang, H.; Glans, P.; Lindle, D. W. *J. Phys. B* **1997**, *30*, 4489.
(22) Perera, R. C. C.; Cowan, P. L.; Lindle, D. W.; LaVilla, R. E.; Jach, T.; Deslattes, R. D. *Phys. Rev. A* **1991**, *43*, 3609.
(23) Abbate, M.; Vicentin, F. C.; Compagnon-Cailhol, V.; Rocha, M. C.; Tolentino, H. *J. Synchrotron Radiat.* **1999**, *6*, 964.
(24) Marinho, R. R. T.; Lago, A. F.; Homem, M. G. P.; Coutinho, L. H.; de Souza, G. G. B.; Naves de Brito, A. *Chem. Phys.* **2006**, *324*, 420.
(25) Willey, W. E. and McLaren, I. W. *Rev. Sci. Instrum.* **1955**, *26*, 1150.
(26) Frisch, M. J.; Trucks, G. W.; Schlegel, H. B.; Scuseria, G. E.; Robb, M. A.; Cheeseman, J. R.; Zakrzewski, V. G.; Montgomery, J. A.; Stratmann, R. E.; Burant, J. C.; Dapprich, S.; Millam, J. M.; Daniels, A. D.; Kudin, K. N.; Strain, M. C.; Farkas, Ö.; Tomasi, J.; Barone, V.; Cossi, M.; Cammi, R.; Mennucci, B.; Pomelli, C.; Adamo, C.; Clifford, S.; Ochterski, J.; Petersson, G. A.; Ayala, P. Y.; Cui, Q, Morokuma, K.; Malick, D. K.; Rabuck, A. D.; Raghavachari, K.; Foresman, J. B.; Cioslowski, J.; Ortiz, J. V.; Baboul, A. G.; Stefanov, B. B.; Liu, G.; Liashenko, A.; Piskorz, P.; Komáromi, I.; Gomperts, R.; Martin, R. L.; Fox, D. J.; Keith, T.; Al-Laham, M. A.; Peng, C. Y.; Nanayakkara, A.; Gonzalez, C.; Challacombe, M.; Gill, P. M. W.; Johnson, B. G.; Chen, W.; Wong, M. W.; Andres, J. L.; Head-Gordon, M.; Replogle, E. S.; Pople, J. A. *GAUSSIAN 03*; Gaussian, Inc.: Pittsburgh, PA, 2003.
(27) Perera, R. C. C.; LaVilla, R. E.; Gibbs, G. V. *J. Chem. Phys.* **1987**, *86*, 4824.
(28) Bodeur, S.; Marechal, J. L.; Reynald, C.; Bazin, D.; Nenner, I. *Z. Phys. D* **1990**, *17*, 291.
(29) Baba, Y.; Yoshii, Y.; Sasaki, T. A. *Surf. Sci.* **1997**, *376*, 330.
(30) Hansen, D. L.; et al. *J. Phys. B* **1999**, *32*, 2629.
(31) James, A. M.; Lord, M. P. *Macmillan's Chemical and Physical Data*; Macmillan: London, 1992.
(32) Eberhardt, W.; Bernstorff, S.; Jochims, H. W.; Whitfield, S. B.; Crasemann, B. *Phys. Rev. A* **1988**, *38*, 3808.
(33) Thomas, T. D.; et al. *J. Phys. B* **1996**, *29*, 3245.
(34) Eland, J. H. D. *Chem. Phys. Lett.* **2005**, *409*, 245.
(35) Zare, R. N. *Mol. Photochem.* **1972**, *4*, 1.
(36) Stöhr, J. *NEXAFS Spectroscopy*; Springer Series in Surface Science, Vol. 25; Springer: Berlin, 1992.
(37) Gel'mukhanov, F.; et al. *Phys. Rev. A* **1998**, *57*, 2511.
(38) Björneholm, O.; et al. *Phys. Rev. Lett.* **2000**, *84*, 2826.
(39) Rosenqvist, L.; et al. *J. Chem. Phys.* **2001**, *115*, 3614.
(40) Simon, M.; Lavollée, M.; Meyer, M.; Morin, P. *J. Electron Spectrosc. Relat. Phenom.* **1996**, *79*, 401.
(41) Lindgren, A.; Gisselbrecht, M.; Burmeister, F. Naves de Brito, A.; Kivimaki, A.; Sorensen, S. L. *J. Chem. Phys.* **2005**, *122*, 114306.
(42) Mocellin, A.; Marinho, R. R. T.; Coutinho, L. H.; Burmeister, F.; Wiesner, K.; Naves de Brito, A. *Chem. Phys.* **2003**, *289*, 163.
(43) Eland, J. H. D. *Acc. Chem. Res.* **1989**, *22*, 281.
(44) Cesar, A.; et al. *J. Chem. Phys.* **1990**, *93*, 918.